

100 ps time-resolved solution scattering utilizing a wide-bandwidth X-ray beam from multilayer optics

K. Ichiyangi,^{a,*} T. Sato,^{a,b} S. Nozawa,^a K. H. Kim,^c J. H. Lee,^c J. Choi,^c A. Tomita,^{a,b} H. Ichikawa,^a S. Adachi,^{a,d} H. Ihee^{c*} and S. Koshihara^{a,b}

^aNon-Equilibrium Dynamics Project, ERATO, Japan Science and Technology Agency, 1-1 Oho, Tsukuba, Ibaraki 305-0801, Japan, ^bTokyo Institute of Technology, 2-12-1 Oh-okayama, Meguro-ku, Tokyo 152-8551, Japan, ^cCenter for Time-Resolved Diffraction, Department of Chemistry, KAIST, Daejeon 305-701, Republic of Korea, and ^dHigh Energy Accelerator Research Organization, 1-1 Oho, Tsukuba, Ibaraki 305-0801, Japan. E-mail: ichiyana@post.kek.jp, hyotcherl.ihee@kaist.ac.kr

100 ps time-resolved X-ray solution-scattering capabilities have been developed using multilayer optics at the beamline NW14A, Photon Factory Advanced Ring, KEK. X-ray pulses with an energy bandwidth of $\Delta E/E = 1\text{--}5\%$ are generated by reflecting X-ray pulses ($\Delta E/E = 15\%$) through multilayer optics, made of W/B₄C or depth-graded Ru/C on silicon substrate. This tailor-made wide-bandwidth X-ray pulse provides high-quality solution-scattering data for obtaining photo-induced molecular reaction dynamics. The time-resolved solution scattering of CH₂I₂ in methanol is demonstrated as a typical example.

Keywords: time-resolved solution scattering; photodissociation reaction; liquidography; multilayers.

1. Introduction

Studying photo-induced reactions in the solution phase with subnanosecond time-resolution offers opportunities for understanding fundamental molecular reaction dynamics in chemistry and biology. Time-resolved X-ray diffraction using 100 ps X-ray pulses from a synchrotron source can elucidate the molecular geometry involved in photo-induced reaction pathways (Plech *et al.*, 2004; Ihee *et al.*, 2005; Georgiou *et al.*, 2006; Davidsson *et al.*, 2005; Kim *et al.*, 2006; Lee *et al.*, 2006, 2008*a,b*; Kong *et al.*, 2007, 2008). An X-ray pulse with $\sim 3\%$ energy bandwidth has been used for solution-scattering experiments at the ID09B beamline of the European Synchrotron Radiation Facility (Plech *et al.*, 2002, 2004; Wulff *et al.*, 2004, 2006; Mirloup *et al.*, 2004; Ihee, 2009). Significant improvements in the signal-to-noise ratios of the experimental data have been reported for photochemical reactions of halogen compounds in solution. For example, the structural dynamics of C₂H₄I₂ in methanol were studied using the high-flux X-ray pulse at the ID09B beamline (Ihee *et al.*, 2005), and the reaction pathways and associated transient molecular structures in solution were resolved by the combination of theoretical calculations and global fitting analysis (Lee *et al.*, 2006; Cammarata *et al.*, 2006).

Recently, beamline NW14A at PF-AR, KEK, was constructed as a 100 ps time-resolved X-ray beamline (Nozawa *et al.*, 2007) using monochromatic or white X-rays. Its high-flux white X-rays have $\Delta E/E \simeq 15\%$ energy bandwidth when an undulator of period length 20 mm is used. To check

the feasibility of time-resolved scattering with such a wide bandwidth and to search for the optimal bandwidth, we simulated the Debye scattering curves for the reaction C₂H₄I₂ → C₂H₄I + I using (i) a 15% bandwidth with the default X-ray energy distribution for the undulator spectrum on NW14A, (ii) a Gaussian spectrum with 5% energy bandwidth, (iii) a Gaussian spectrum with a 1% energy bandwidth, and (iv) a Gaussian spectrum with 0.01% energy bandwidth, as shown in Fig. 1. The photon flux of the X-ray pulse increases with the energy bandwidth, but the simulation shows that the 15% energy bandwidth with the default spectrum with a long tail is not suitable for time-resolved solution-scattering experiments owing to insufficient *q*-resolution. The long tail of the default X-ray spectrum induces a much higher extent of blurring at high scattering angles than a symmetric Gaussian spectrum with the same bandwidth. For this reason, the X-ray spectrum with a long tail at ID09B of ESRF with $\sim 3\%$ bandwidth is comparable with a Gaussian spectrum with $\sim 10\%$ bandwidth. In contrast, when we compare the calculated scattering curve using the Gaussian spectrum with 1% and 5% energy bandwidth X-rays with that with a 0.01% energy bandwidth, three calculated curves seem to reproduce the same quality. In addition, the total flux of the 5% energy bandwidth X-ray beam will be higher than that of the monochromatic X-rays ($\sim 0.01\%$ energy bandwidth) from a Si single crystal by a factor of 250. The total flux of the 5% energy bandwidth X-rays is about five times more than that of the 1% energy bandwidth X-rays. Therefore, the data collecting time using the 5% energy bandwidth X-rays becomes shorter than when

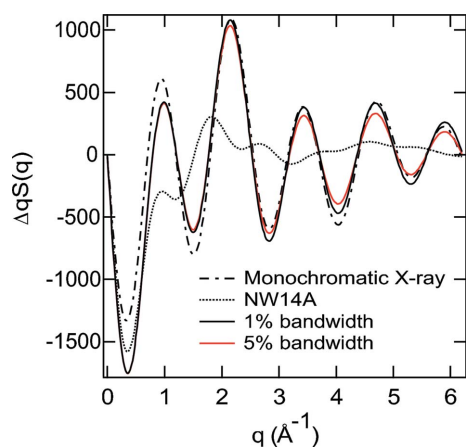


Figure 1
Debye scattering curves calculated for the model reaction $C_2H_4I_2 \rightarrow C_2H_4I + I$ using a 0.01% (monochromatic) Gaussian X-ray energy profile (dot-dashed line), 5% Gaussian X-ray energy profile (red line), 1% Gaussian X-ray energy profile with a long tail (dotted line), and 15% default X-ray energy profile with a long tail (solid line).

using the monochromatic X-rays and the 1% energy bandwidth X-rays. These estimations clearly indicate that the preparation of X-ray pulses with $\Delta E/E \simeq 5\%$ has a very significant merit for promoting a time-resolved X-ray solution-scattering experiment, and, thus, prompted us to reduce the bandwidth from the default 15% down to less than the $\sim 5\%$ energy bandwidth of multilayer optics.

In our experimental set-up, the multilayer optics can produce X-rays with a 1–5% energy bandwidth, and allow us to measure the time-resolved solution-scattering with the undulator at the NW14A beamline. The purpose of this paper is to present a detailed account of achievements with the multilayer optics. We succeeded in collecting high-quality time-resolved solution-scattering data for the CH_2I_2 photo-

chemical reaction in methanol and briefly report the experimental aspects.

2. Experimental set-up

A schematic diagram of the experimental set-up is shown in Fig. 2. The experimental system consists of an amplified Ti:sapphire laser system for providing laser pulses to excite the liquid sample, an X-ray pulse selector (XPS) to select single X-ray pulses, a heat-load chopper (Gembicky *et al.*, 2007), laser and X-ray shutters, and a sapphire nozzle to provide a stable liquid jet. This beamline gives a white X-ray pulse in the energy range 13–18 keV using an undulator with a period length of 20 mm at a repetition rate of 794 kHz and with a pulse duration of about 100 ps. The scattered images were recorded on an integrating charge-coupled device detector (MarCCD165, MarUSA) of diameter 165 mm. Details of the set-up have been described elsewhere (Nozawa *et al.*, 2007).

3. Production of a wide-bandwidth X-ray beam using multilayer optics

We have utilized two types of multilayer optics. The first one is W/B₄C ($d = 27.7 \text{ \AA}$, X-ray Company, Russia) on a Si single crystal with a size of $50 \times 50 \times 5 \text{ mm}$, which provides an X-ray spectrum with $\sim 1\%$ energy bandwidth and in which the peak energy of the X-ray spectrum can be changed by tilting the angle of the multilayer optics, as shown in Fig. 3(a). The second multilayer, which is a depth-graded Ru/C layer ($d = 40 \text{ \AA}$, NTT Advanced Technology, Japan), produces a $\sim 5\%$ energy bandwidth from the undulator spectrum, as shown in Fig. 3(b). A real image of the multilayer mirror installed in the

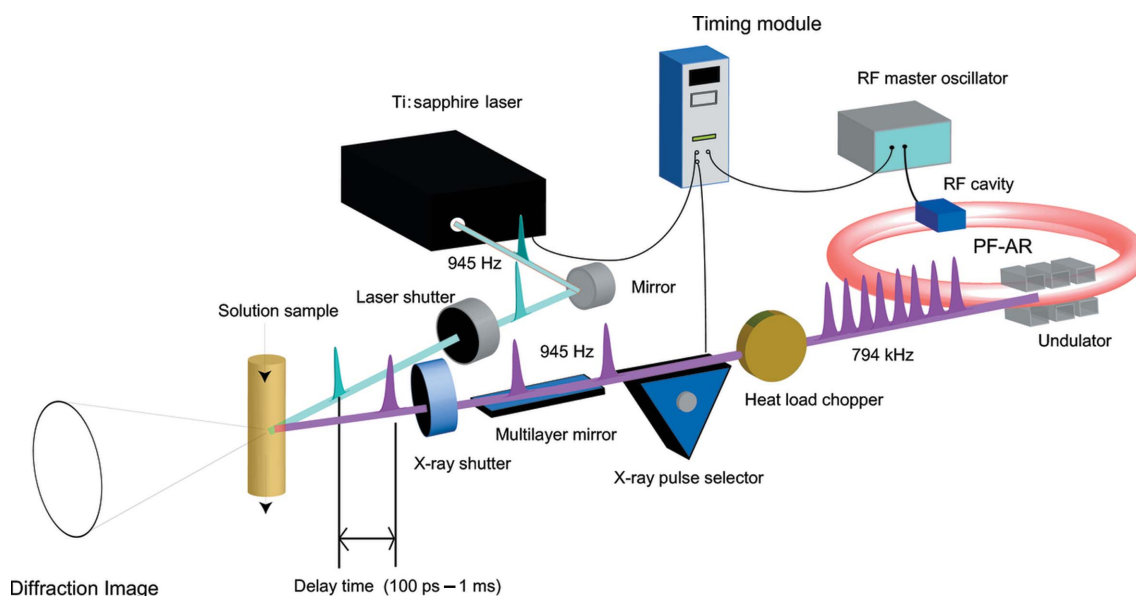


Figure 2
Schematic diagram of the time-resolved solution X-ray scattering at beamline NW14A, PF-AR. The wide-bandwidth ($\Delta E/E = 1\text{--}5\%$) X-ray pulses at 945 Hz are provided from the multilayer optics downstream of the X-ray pulse selector. The laser and the X-ray pulse selector are synchronized by using the RF master oscillator.

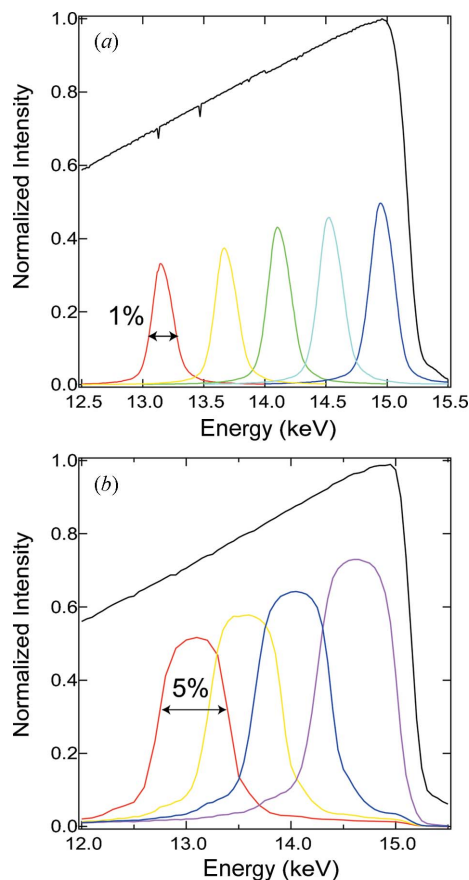


Figure 3

Wide-bandwidth X-ray pulses were produced by multilayer optics from the undulator spectrum. The peak energy position is controlled by changing the incident angle. The black curve is the X-ray spectrum from the undulator, with a gap of 11 mm. (a) X-ray spectra using the W/B₄C multilayer optics. The X-ray bandwidth is about 1%. (b) X-ray spectra using the depth-graded Ru/C multilayer optics. The X-ray bandwidth is 5%.

vacuum chamber is shown in Fig. 4. The diameter of the vacuum chamber placed on a swivel stage is 160 mm. The multilayer optics is mounted on a water-cooled copper holder. A white X-ray pulse with a photon flux of 1×10^9 photons per pulse is produced in the energy range at a 1 kHz repetition rate with the XPS. When multilayer optics with 1% and 5% energy bandwidths are used downstream of the XPS, the photon fluxes are 6×10^7 and 3×10^8 photons per pulse, respectively. We can use the discretionary wavelengths and bandwidth in the X-rays for spectra, which is an advantage for the scattering curve corresponding to the asymmetric undulator spectra.

4. Time-resolved solution scattering of CH₂I₂

Photo-induced chemical and biological reactions have been extensively studied by time-resolved spectroscopic techniques and theoretical calculations. Time-resolved X-ray solution scattering makes it possible to probe transient molecular structures in the photo-induced reactions. We measured the time-resolved scattering signals for photodissociation of the iodine atom from CH₂I₂ in methanol (Davidsson *et al.*, 2005).

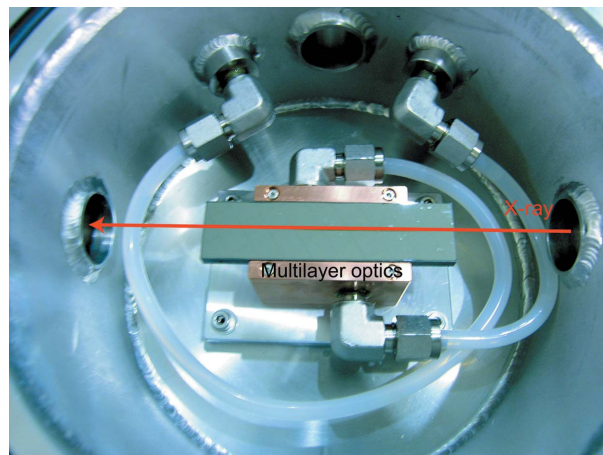


Figure 4

The depth-graded Ru/C multilayer in the vacuum chamber installed at the NW14A beamline at the Photon Factory Advanced Ring at KEK. The multilayer is mounted on a water-cooled holder.

We performed the measurement using X-rays with 5% energy bandwidth at 18 keV to evaluate the feasibility of this set-up. The 60 mM CH₂I₂ (Aldrich, Japan) in methanol solution was flowed using a liquid jet of thickness 0.3 mm at a flow rate of about 3 m s^{-1} . The open jet makes it possible to remove any background signal owing to the scattering of a glass capillary. The CH₂I₂ in methanol solution was excited by 267 nm light, the third harmonic of the Ti:sapphire femtosecond laser system. To ensure one-photon absorption, the laser pulse width was stretched to ~ 2 ps by passing 150 fs laser pulses through a fused silica glass rod cut at the Brewster angle for 267 nm with 175 mm optical length. The spot size of both the X-ray and laser beams on the sample surface was 200 μm diameter. The laser path was set almost parallel to the X-ray path ($\sim 10^\circ$ tilt), and the intensity of the laser beam on the sample surface was adjusted to $\sim 35 \mu\text{J}$ per pulse. The sample-to-CCD distance and the exposure time were 48.6 mm and 7 s per image, respectively. The CCD detector allowed a 2θ angle range from about 3 to 62° to be measured. Difference diffraction data were measured at time delays of -200 ps, 100 ps, 300 ps, 1 ns, 3 ns, 10 ns, 30 ns, 50 ns, 100 ns, 300 ns and 1 μs , as shown in Fig. 5. The CCD images were converted to one-dimensional curves using the FIT2D program (<http://www.esrf.eu/computing/scientific/FIT2D/>). To extract the diffraction intensity change alone, the data for an unperturbed sample at -3 ns were subtracted from the diffraction data collected at other time delays. Photo-induced heating of the solvent is evident in the low q region ($\leq 2 \text{ \AA}^{-1}$). The change in the high q region indicates the photo-induced structural changes of the CH₂I₂ molecule. Details of the data analysis will be reported elsewhere.

5. Conclusion

Wide-bandwidth X-ray pulses were generated from depth-graded Ru/C and W/B₄C multilayer optics for time-resolved X-ray solution scattering. The symmetric shape and the

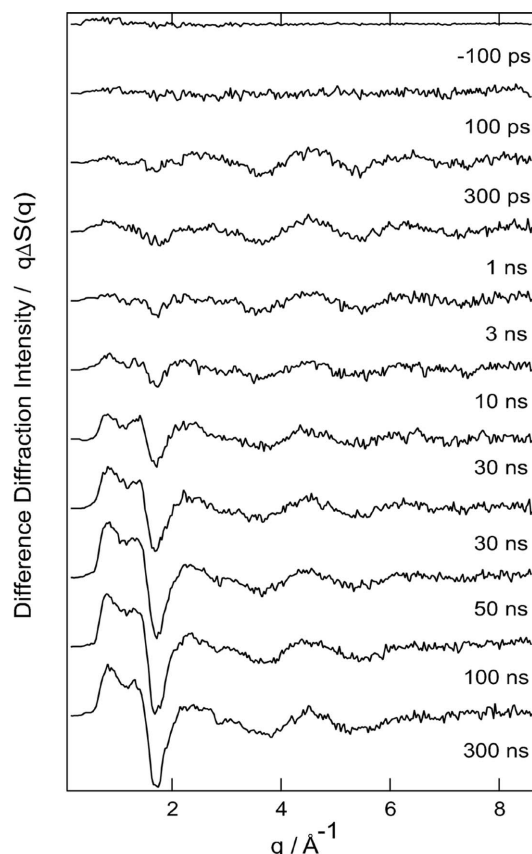


Figure 5
Subnanosecond time-resolved diffraction signal of CH_2I_2 in methanol solution as a function of time delay. The differential diffraction intensity was obtained by subtracting the diffraction signal at a reference negative time delay (-3 ns) from the diffraction signal at each time delay.

bandwidth ($\Delta E/E = 1\text{--}5\%$) of the energy spectra of the X-ray pulse are suitable for time-resolved solution-scattering experiments, and quantitative analysis of photo-induced molecular reaction dynamics in solution. We successfully measured the solution scattering from CH_2I_2 in methanol and the time dependence of the difference scattering was presented.

We are grateful to Michael Wulff (ESRF), Atsuo Iida and Hiroshi Kawata (Photon factory, KEK) for discussions of the multilayer optics. We also thank Philip Coppens and Milan Gembicky (State University of New York at Buffalo) for the

use of the heat-load chopper. This work was performed under the approval of the Photon Factory Advisory Committee (Proposal No. 2004S1-001) and supported by National Creative Research Initiatives (Center for Time-Resolved Diffraction) of MEST/KOSEF.

References

- Cammarata, M., Lorec, M., Kim, T. K., Lee, J. H., Kong, Q. Y., Pontecorvo, E., Russo, M., Schiró, G., Cupane, A., Wulff, M. & Ihee, H. (2006). *J. Chem. Phys.* **124**, 124504.
- Davidsson, J., Poulsen, J., Cammarata, M., Georgiou, P., Wouts, R., Katona, G., Jacobson, F., Plech, A., Wulff, M., Nyman, G. & Neutze, R. (2005). *Phys. Rev. Lett.* **94**, 245503.
- Gembicky, M., Adachi, S. & Coppens, P. (2007). *J. Synchrotron Rad.* **14**, 295–296.
- Georgiou, P., Vincent, J., Anderson, M., Annemarie, W. B., Gourdon, P., Poulsen, J., Davidsson, J. & Neutze, R. (2006). *J. Chem. Phys.* **124**, 234507.
- Ihee, H. (2009). *Acc. Chem. Res.* **42**, 356–366.
- Ihee, H., Lorenc, M., Kim, T. K., Kong, Q. Y., Cammarata, M., Lee, J. H., Bratos, S. & Wulff, M. (2005). *Science*, **209**, 1223–1227.
- Kim, T. K., Lorenc, M., Lee, J. H., Russo, M., Kim, J., Cammarata, M., Kong, Q., Noel, S., Plech, A., Wulf, M. & Ihee, H. (2006). *Proc. Natl. Acad. Sci. USA*, **103**, 9410–9415.
- Kong, Q., Lee, J. H., Plech, A., Wulff, M., Ihee, H. & Koch, M. H. J. (2008). *Angew. Chem. Int. Ed.* **47**, 5550–5553.
- Kong, Q., Wulff, M., Lee, J. H., Bratos, S. & Ihee, H. (2007). *J. Am. Chem. Soc.* **127**, 13584–13590.
- Lee, J. H., Kim, H. K., Kim, T. K., Lee, Y. & Ihee, H. (2006). *J. Chem. Phys.* **125**, 172504.
- Lee, J. H., Kim, J., Cammarata, M., Kong, Q., Kim, K. H., Choi, J., Kim, T. K., Wulff, M. & Ihee, H. (2008a). *Angew. Chem. Int. Ed.* **47**, 1047–1050.
- Lee, J. H., Kim, T. K., Kim, J., Kong, Q., Cammarata, M., Lorenc, M., Wulff, M. & Ihee, H. (2008b). *J. Am. Chem. Soc.* **130**, 5834–5835.
- Mirloup, F., Vuilleumier, R., Bratos, S., Wulff, M. & Plech, A. (2004). *Femtochemistry and Femtobiology*, edited by M. Martin and J. T. Hynes. New York: Wiley.
- Nozawa, S. *et al.* (2007). *J. Synchrotron Rad.* **14**, 313–319.
- Plech, A., Randler, R., Geis, A. & Wulff, M. (2002). *J. Synchrotron Rad.* **9**, 287–292.
- Plech, A., Wulff, M., Bratos, S., Mirloup, F., Vuilleumier, R., Schotte, F. & Anfinrud, P. A. (2004). *Phys. Rev. Lett.* **92**, 125505.
- Wulff, M., Bratos, S., Plech, A., Vuilleumier, R., Mirloup, F., Lorenc, M., Kong, Q. Y. & Ihee, H. (2006). *J. Chem. Phys.* **124**, 034501.
- Wulff, M., Lorenc, M., Plech, A., Ihee, H., Bratos, S., Mirloup, F. & Vuilleumier, F. (2004). *Femtosecond and Femtobiology*, edited by M. Martin and J. T. Hynes. New York: Wiley.